Journal of Applied Mechanics and Technical Physics, Vol. 36, No. 1, 1995

FRICTION AND MASS TRANSFER IN TRANSVERSE FLOW AROUND A CYLINDER IN A GRANULAR BED AND A NARROW SLOT

A. V. Gorin, A. V. Zarubin, T. N. Mikhailova, V. A. Mukhin, and D. F. Sikovskii

UDC 532.446+536.24

Introduction. The problem of computing the thermal conditions for bodies immersed in an infiltrated granular bed is of interest in many areas of thermal power engineering and chemical technology. The traditional approach to solving this problem is to use the average heat transport equations and Darcy's law of filtration neglecting the condition for fluid sticking to the wall. The potential character of the flow allows us to find rather simple analytical dependences for the heat transfer [1]. The results obtained in this way are valid for filtration velocities which are not too high, as long as thethermal boundary layer is thick enough so we can neglect the effect of the wall zone of the granular layer. For high Peclet numbers, the thermal boundary layer is localized within the wall zone, and we need to use other approaches to solving this problem.

The simplest model for flow in a problem medium, taking into account the condition for sticking to the wall, is the model in [1]

$$\frac{\mu}{m}\nabla^2\mathbf{v} - \frac{\mu}{K}\mathbf{v} - \nabla p = 0; \tag{1}$$

$$\nabla \cdot \mathbf{v} = 0, \tag{2}$$

where v is the filtration velocity; μ is the velocity of the fluid; p is the pressure; K, m are the permeability and porosity of the granular bed. As shown in [3], the tangential stress on the wall of a tube with a granular bed calculated using model (1), (2) proved to be in good agreement with the experimental data.

Heat transfer in a porous medium is modeled using the heat transport equation with effective thermal conductivity coefficient

$$\mathbf{v} \cdot \nabla T = a_{ef}\nabla^2 T \tag{3}$$

(T is the average temperature of the medium).

Equations (1)-(3) are similar to the equations of average motion in a narrow gap between two plane-parallel plates, or in a Hele–Shaw cell [4]. Assuming no transverse motion and parabolicity of the local velocity distribution

$$\mathbf{w}(x, y, z) = 6\frac{z}{h}\left(1 - \frac{z}{h}\right)\mathbf{v}(x, y)$$

(w, v are the local and average flow velocity vectors, lying in the Oxy plane parallel to the plates of the cell; z is the transverse coordinate ($0 \le z \le h$)), averaging the Stokes equations over the width of the gap

$$\mu\nabla^2\mathbf{w} + \mu\frac{\partial^2\mathbf{w}}{\partial z^2} - \nabla p = 0, \frac{\partial p}{\partial z} = 0, \nabla \cdot \mathbf{w} = 0$$

($\nabla = (\partial/\partial x, \partial/\partial y)$) leads to the following system of equations of motion:

Novosibirsk. Translated from Prikladnaya Mekhanika i Tekhnicheskaya Fizika, No. 1, pp. 112-121, January-February, 1995. Original article submitted July 15, 1993. Revision submitted February 28, 1994.

0021-8944/95/3601-0105$12.50

$$\mu \nabla^2 \mathbf{v} - \frac{12\mu}{h^2} \mathbf{v} - \nabla p = 0; \tag{4}$$

$$\nabla \cdot \mathbf{v} = 0. \tag{5}$$

If we assume that the local temperature distribution over the cross section of a cell whose side plates are thermally insulated is constant (T = T(x, y)), then averaging of the heat transport equation over the cross section of the slot gives

$$\mathbf{v} \cdot \nabla T = a \nabla^2 T \tag{6}$$

(a is the thermal conductivity of the fluid).

The similarity of equations (1), (2), to equations (4), (5) and also the similarity of (3) to (6) allows us to hope that using a Hele–Shaw cell we can model heat and mass transfer processes in a porous medium for large Peclet numbers. Such modeling has significant advantages over making direct measurements in a porous medium, requiring fine and tedious experimental technique minimally disturbing the structure of the medium. The possibilities for hydrodynamic and thermal visualization are considerably increased. Furthermore, when modeling using a Hele–Shaw cell, the transfer coefficients and the properties of the fluid are known, while in a porous medium we need additional measurements of the effective transfer coefficients. In [5, 6], an analogy was demonstrated between heat transfer processes for natural convection in a porous medium and in a Hele–Shaw cell.

In this paper, we have carried out a theoretical and experimental investigation of mass transfer to a cylinder in a Hele–Shaw cell for forced convection. The results obtained are compared with analogous experiments in a granular bed carried out earlier. We have demonstrated the analogy between the processes of convective heat and mass transfer in a porous medium and in a Hele–Shaw cell for large Peclet numbers Pc.

Hydrodynamics and Mass Exchange in Flow Around a Cylinder in a Hele–Shaw Cell. Let us consider flow around a cylinder of radius R (located transverse to a narrow slot formed by two plane-parallel plates) by a uniform flow of fluid with average flow velocity U_∞. After introducing the stream function Eqs. (4), (5) are transformed.

$$\nabla^4 \psi - \frac{12}{h^2} \nabla^2 \psi = 0. \tag{7}$$

The boundary conditions for uniformity of flow far from the cylinder and sticking on its boundary have the form

$$\psi \to U_\infty r \sin\theta, \quad r \to \infty,$$

$$\psi = 0, \frac{\partial \psi}{\partial r} = 0, \quad r = R \tag{8}$$

(r, θ are the polar coordinates).

Problem (7), (8) is easily solved by the method of separation of variables:

$$\psi = U_\infty \left[r - \frac{K_2(2\sqrt{3}R/h)}{K_0(2\sqrt{3}R/h)} \frac{R^2}{r} + \frac{hK_1(2\sqrt{3}r/h)}{\sqrt{3}K_0(2\sqrt{3}R/h)} \right] \sin\theta. \tag{9}$$

From (9) we find the tangential stress of friction on the surface of the cylinder

$$\tau = \mu \frac{\partial^2 \psi}{\partial r^2}\Big|_{r=R} = 4\sqrt{3} \frac{\mu U_\infty}{h} \frac{K_1(2\sqrt{3}R/h)}{K_0(2\sqrt{3}R/h)} \sin\theta. \tag{10}$$

For Hele–Shaw flows, a typical situation is when the longitudinal dimensions of the body considerably exceed the thickness of the slot (R >> h). In this case, the ratio of the MacDonald functions in (1) is practically unity, therefore

$$\tau = 4\sqrt{3} \frac{\mu U_\infty}{h} \sin\theta = 6{,}928 \frac{\mu U_\infty}{h} \sin\theta. \tag{11}$$

Analogously to (6), the equation for the concentration has the form

$$\mathbf{v} \cdot \nabla C = D \nabla^2 C \tag{12}$$

(D is the diffusion coefficient). On the surface of the cylinder, we impose a boundary condition of the first kind

$$C = C_w, \; r = R \tag{13}$$

(C_w is the concentration on the surface). Far from the cylinder, the concentration tends toward the concentration of the substance in the incoming flow:

$$C \to C_\infty, \; r \to \infty. \tag{14}$$

Let us solve problem (12)-(14) in the approximation of a diffusion boundary layer, assuming it is so thin that the distribution of the longitudinal velocity within the limits of the diffusion layer is linear:

$$u = \frac{\tau}{\mu} y. \tag{15}$$

Then let us use the boundary-layer coordinates tied to the surface of the cylinder y = r — R, x = rθ. From the continuity equation and expression (15), it is easy to obtain an expression for the y component of the velocity

$$v = -\frac{1}{2\mu} \frac{d\tau}{dx} y^2.$$

Then the equation for the diffusion boundary layer is written as follows:

$$\frac{\tau}{\mu} y \frac{\partial C}{\partial x} - \frac{1}{2\mu} \frac{d\tau}{dx} y^2 \frac{\partial C}{\partial y} = D \frac{\partial^2 C}{\partial y^2}; \tag{16}$$

$$C = C_w, \; y = 0, \; C = C_\infty, \; y \to \infty. \tag{17}$$

The problem (16), (17) has the known solution [7]:

$$\frac{C - C_w}{C_\infty - C_w} = \frac{3}{\Gamma\left(\frac{1}{3}\right)} \int_0^\eta e^{-t^3} dt. \tag{18}$$

Here

$$\eta = \frac{y\tau^{1/2}(x)}{[9\mu D \int_0^x \tau^{1/2}(x')dx']^{1/3}}. \tag{19}$$

Let us define the Sherwood number as

$$\mathrm{Sh} = \frac{j_w 2R}{D(C_w - C_\infty)}$$

($j_w = -D\partial C/\partial y \mid_{y=0}$ is the diffusion flux on the surface of the cylinder). Using relations (11), (18), (19), for the local Sherwood number we obtain

$$\mathrm{Sh}(\theta) = \frac{3^{1/2} \cdot 2^{4/3}}{\Gamma\left(\frac{1}{3}\right)} \left(\mathrm{Pe} \frac{R}{h}\right)^{1/3} \Phi(\theta) = 1{,}629 \left(\mathrm{Pe} \frac{R}{h}\right)^{1/3} \Phi(\theta), \tag{20}$$

where

$$\Phi(\theta) = \sin^{1/2}\theta\left[\int_0^\theta \sin^{1/2}t\,dt\right]^{-1/3};\ \mathrm{Pe} = \frac{2U_\infty R}{D}.$$

The value of Sh at any ($\theta = 0$) point of the cylinder and the average value of Sh respectively have the form

$$\mathrm{Sh}_{fr} = \mathrm{Sh}(0) = \frac{2\cdot 3^{5/6}}{\Gamma\left(\frac{1}{3}\right)}\left(\mathrm{Pe}\frac{R}{h}\right)^{1/3} = 1{,}865\left(\mathrm{Pe}\frac{R}{h}\right)^{1/3}; \tag{21}$$

$$\mathrm{Sh}_m = \frac{1}{\pi}\int_0^\pi \mathrm{Sh}(\theta)d\theta = \frac{3}{2\pi}\left[\pi^{1/2}\frac{\Gamma\left(\frac{3}{4}\right)}{\Gamma\left(\frac{5}{4}\right)}\right]^{2/3}\frac{3^{1/2}\cdot 2^{4/3}}{\Gamma\left(\frac{1}{3}\right)}\left(\mathrm{Pe}\frac{R}{h}\right)^{1/3} = 1{,}393\left(\mathrm{Pe}\frac{R}{h}\right)^{1/3}. \tag{22}$$

For a cylinder in a porous medium, we write Eqs. (7) and (12) as

$$\nabla^4\psi - \frac{m}{K}\nabla^2\psi = 0,\ \mathbf{v}\cdot\nabla C = D_{\mathrm{eff}}\nabla^2 C$$

(D_{eff} is the effective diffusion coefficient), and we represent the solutions obtained above as follows:

$$\tau = \frac{2\mu U_\infty m^{1/2}}{K^{1/2}}\sin\theta; \tag{23}$$

$$\mathrm{Sh}(\theta) = 0{,}855\mathrm{Pe}^{1/3}\left(\frac{m}{\mathrm{Da}}\right)^{1/6}\Phi(\theta); \tag{24}$$

$$\mathrm{Sh}_{fr} = 0{,}978\mathrm{Pe}^{1/3}\left(\frac{m}{\mathrm{Da}}\right)^{1/6}; \tag{25}$$

$$\mathrm{Sh}_m = 0{,}731\mathrm{Pe}^{1/3}\left(\frac{m}{\mathrm{Da}}\right)^{1/6}. \tag{26}$$

Here the Sherwood and Peclet numbers include the effective diffusion coefficient D_{eff}; the Darcy number $\mathrm{Da} = k/(2R)^2$.

Earlier the problem of flow around a cylinder was solved in a full three-dimensional formulation in [8] using the method of joining asymptotic expansions about the small parameter h/R. The inner expansion of the velocity along the boundary of the cylinder, valid at distances O(h) from the boundary, has the form [8]

$$u^{(i)} = 2U_\infty\sin\theta\left\{6\frac{z}{h}\left(1-\frac{z}{h}\right) - \frac{48}{\pi^3}\sum_{k=0}^{\infty}(2k+1)^{-3}\sin\left[\pi(2k+1)\frac{z}{h}\right]e^{-\pi(2k+1)\frac{y}{h}}\right\}.$$

From this, the tangential frictional stress averaged over the cross section of the slot is

$$\tau = \frac{1}{h}\int_0^h \mu\left.\frac{\partial u^{(i)}}{\partial y}\right|_{y=0} dz = \frac{168\zeta(3)}{\pi^3}\frac{\mu U_\infty}{h}\sin\theta = 6{,}513\frac{\mu U_\infty}{h}\sin\theta,$$

which is different from the result (11) we obtained by 6.4%. Yielding results which are insignificantly different from the more exact solution in [8], the proposed method for solving the problem using equations averaged over the cross section of the slot is considerably simpler (the two-dimensional problem is solved). At the same time, the average equations of motion and heat and mass transport in the Hele–Shaw cell are similar to analogous transport equations in porous media, which makes it possible to use a Hele–Shaw call for modeling forced convection in a porous medium for large Peclet numbers.

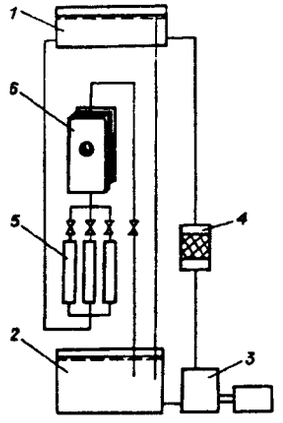

Fig. 1

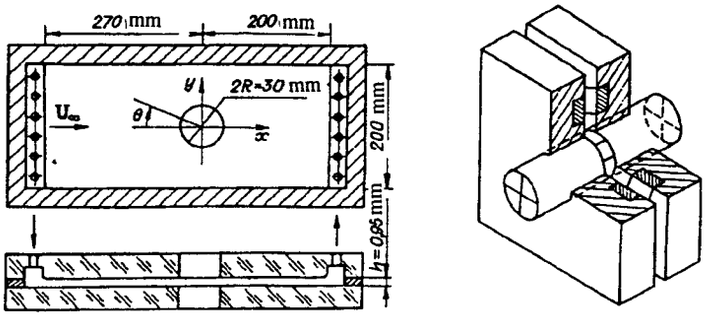

Fig. 2

Description of the Experimental Apparatus and Technique. We used the electrodiffusion method in [9] for measurement of the mass exchange. The apparatus was a closed circulating loop with a reservoir at a constant level 1 (Fig. 1). The electrolyte from the lower reservoir 2 was supplied to the upper constant-level reservoir by pump 3 through a thin purification filter 4. The fluid was supplied to the working section 6 from the upper reservoir through the system of rotameters 5, and then ran into the lower reservoir 2. The working section (Fig. 2) was made of two organic glass plates of thickness 24 mm, between which an insert of organic glass of thickness 0.95 mm was pressed along the edges. The geometric dimensions of the section and the experimental cylinder (2R = 30 mm) matched the dimensions of analogous elements in [10].

A schematic diagram of the experimental cylinder also is shown in Fig. 2. The working surface of the cylinder (the cathode) consisted of two parts: the smaller part served for measurement of the local mass exchange. The anode is two rings made flush with the surface on the side walls of the channel. The cylinder can be rotated about the axis.

Thus, using a local sensor, we could obtain the distribution of the mass exchange coefficient along the perimeter of the cylinder. The dimension of the local sensor along the course of the flow (along the perimeter of the cylinder) is 1.9 mm. The gap between sensors was only 0.1 mm. The transverse dimension of the sensors matched the transverse dimension of the channel (0.95 mm). The total mass flux from the entire surface of the cylinder could be obtained by two methods integration of the readings of the local sensor and simultaneous measurement using the large and small sensors, which allowed us to monitor the quality of the experiments.

The working fluid was a 0.02 normal solution of potassium ferricyanide and a 0.024 normal solution of potassium ferrocyanide in a 0.6 normal aqueous NaOH solution. The electrolyte solution differed little from water with respect to its physical properties. The mass transfer coefficient was determined using the formula $\beta = I/(nFSC_0)$, where I is the limiting diffusion current of the sensor, A; n is the number of electrons participating in the electrochemical reaction (for the ferricyanide system, n = 1); F is the Faraday number, F = 96,500 coulombs/mole; S is the area of the sensor, m^2; C_0 is the concentration f active $[Fe(CN)_6]^{3-}$ ions in solution, moles/m^3. For determination of the diffusion coefficient, we used the dependence [11]

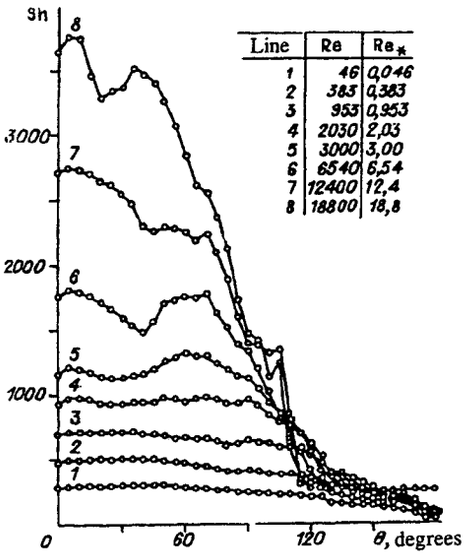

Fig. 3

$$\frac{\mu D}{T} = (2{,}34 + 0{,}14\Gamma_0) \cdot 10^{-15}.$$

Here $\Gamma_0 = 0.5\sum_{i=1}^{n} Z_i C_i$ is the ionic strength of the solution; Z_i is the charge on the ions comprising the electrolyte; C_i is their concentration in solution, moles/m^3. The viscosity of the electrolyte was determined by VPZh-3 viscometer, the concentration of $[Fe(CN)_6]^{3-}$ ions was determined by a spectrophotometer, the temperature of the solution was determined using a thermocouple, and the electric current was measured by a microammeter. The fluid flow rate was monitored by a system of precalibrated rotameters. The range of investigated Reynolds numbers Re in the apparatus was determined ultimately by the ratio of the rate at which ions were supplied to the surface and the rate of the chemical reaction. The quality of the voltage–current curves deteriorated at large Reynolds numbers.

Discussion of Experimental Results. In Fig. 3, we present the experimentally measured distributions of the mass transfer coefficient over the surface of the cylinder. In Fig. 4, they are compared with the values calculated using expression (20). All the way up to $Re = 2U_\infty R/\nu \approx 600$, we observe satisfactory agreement between the measured quantities and the calculated values. With further increase in Re, the measured values become higher than the calculated values in the front part of the cylinder ($0 < \theta < 90°$) and the mass transfer rate in the back portion of the cylinder ($90° < \theta < 180°$) becomes practically constant. The latter phenomenon is connected with development of a backflow zone to the rear of the cylinder [10] under the action of inertial forces. A measure of their effect is the ratio of the characteristic value of the convective terms $\rho U_\infty^2(2R)$ (in Eq. (4), they are discarded) to the scale of the drag force in the Hele–Shaw cell $\mu U_\infty/h^2$ (see (4)), i.e., the Reynolds number

$$Re_* = \frac{U_\infty h^2}{2\nu R} = Re\left(\frac{h}{2R}\right)^2,$$

the values of which are indicated in Figs. 3 and 4 along with the conventional Reynolds number Re. For the given experimental conditions, $Re_* = 10^{-3} \cdot Re$, thus deviation of the mass transfer value from the calculated formulas obtained above occurs for $Re_* = 0.6$.

The experimental result presented in Figs. 5 and 6 ($Sc = \nu/D$ is the Schmidt number) on the mass transfer at any point and the average mass transfer also deviate from the calculated dependences for $Re_* = 0.6$. Thus the value $Re_* = 0.6$ delimits the range of applicability of the solutions presented above for the average transport equations in a Hele–Shaw cell.

In order to illustrate the analogy between transport processes in a porous medium and in a Hele–Shaw cell, let us compare the calculated dependences (23)-(26) with the experimental measurements of the friction and mass transfer for trans-

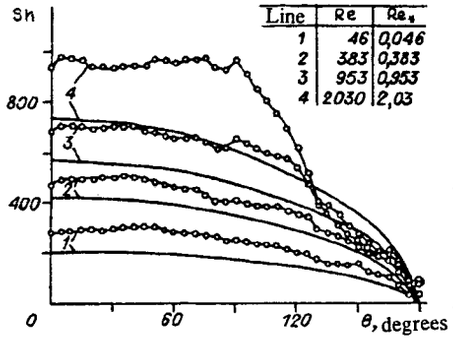

Fig. 4

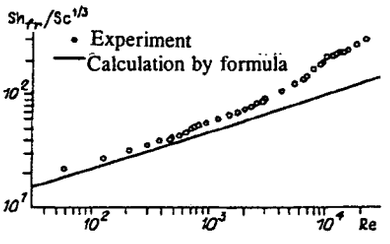

Fig.5

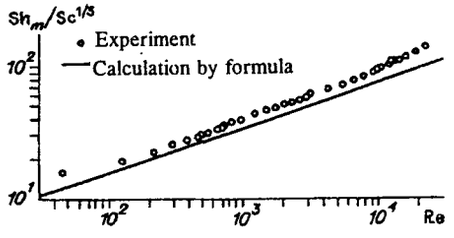

Fig. 6

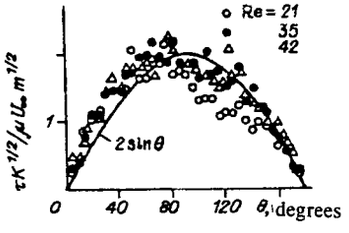

Fig. 7

verse flow around a cylinder in a granular bed, carried out using the electrodiffusion method in [12, 13]. In the experiments, we used a cylinder of diameter 2R = 50 mm and glass beads of diameter d_p = 3.2 mm. The permeability of the granular bed was calculated using the Carmen–Kozeny formula

$$K = \frac{m^3 d_p^2}{180(1-m)^2}$$

for porosity m = 0.4 for random packing of spheres [14].

In Fig. 7, we present experimental data from [12] on the distribution of the dimensionless tangential frictional stress over the surface of the cylinder

$$\bar{\tau} = \frac{\tau K^{1/2}}{\mu U_\infty m^{1/2}}$$

for different filtration velocities compared with its theoretical value $2\sin\theta$ (the line) according to (23). In Fig. 8, we present the average coefficient of friction

$$c_f = \frac{2\bar{\tau}}{\rho_f U_\infty^2} = \frac{2}{\pi\rho_f U_\infty^2}\int_0^\pi \tau(\theta)d\theta$$

compared with the calculated dependence following from (23)

$$c_f = \frac{8}{\pi}\frac{\nu_f m^{1/2}}{U_\infty K^{1/2}} = \frac{8m^{1/2}}{\pi}(\mathrm{ReDa})^{-1}, \tag{27}$$

where ρ_f, ν_f are the density and viscosity of the fluid; m = 0.4; Da = $4.1\cdot10^{-6}$ for the given experimental conditions.

As we see from this graph satisfactory agreement between the calculation and the experimental is observed up to Re $\approx 2U_\infty R/\nu_f \approx 60$, after which the experimental points go below the theoretical curve; Re $\approx$ 60 under the given experimental conditions corresponds to a Reynolds number along the diameter of the grain to $Re_p = U_\infty d_p/\nu_f \approx 3$. For such values of Re_p,

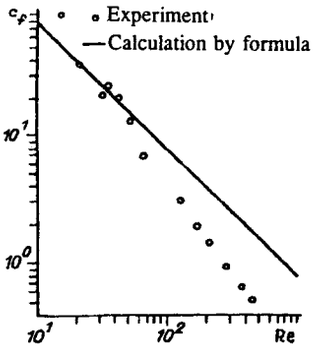

Fig. 8

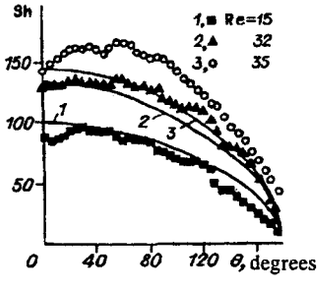

Fig. 9

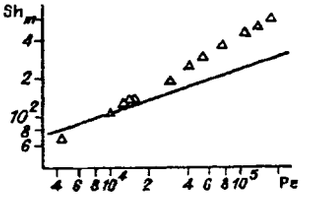

Fig. 10

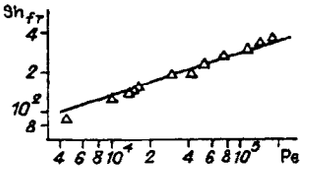

Fig. 11

rearrangement of the flow regime in the granular bed occurs: the slow Darcy filtration flow regime changes to the inertial regime with development (under the action of growing inertial forces) of separation zones in the flow of fluid between grains [15].

Due to the absence of experimental information about the effective diffusion coefficient, we have assumed the following expression for it:

$$D_{\text{eff}} = 3{,}0D_f, \tag{28}$$

where D_f is the diffusion coefficient for the liquid.

The consistency of the results of measurements of the local mass transfer coefficient presented in Fig. 9 with the values calculated using formulas (24) and (28) (lines 1-3) also can be considered satisfactory up to values of Re $\approx$ 40 ($Re_p \approx 2$), for which deviation of the experimental data [13] from the calculated values occurs. An analogous pattern occurs in the behavior of the average mass transfer coefficient (Fig. 10, where the points represent the experimental results from [13], the line represents the calculation using formulas (26) and (28)).

As we see, deviation from the calculation dependences occurs at approximately the same values of Re_p as for the friction. In this case, enhancement of mass tranfer occurs upon going to the inertial flow regime in a granular bed compared with the Darcy filtration regime.

The measured mass transfer coefficient at any point of the cylinder agrees satisfactorily with the calculation using (25) and (28) (the line) over the entire range of filtration velocities, as we see from Fig. 11 (the points represent the experimental results in [13]). This is connected with the low velocities of motion of the fluid in its vicinity and consequently with the later transition to the inertial flow regime.

Thus the presented analysis of the experimental data on mass exchange transverse to a cylinder in a granular bed with flow around the cylinder and in a Hele–Shaw cell has demonstrated the existence of an analogy between these two processes up to $Re_p \approx$ 2-3 in a granular bed and $Re_* \approx 0.6$ in a narrow slot.

REFERENCES

1. Yu. A. Buevich and D. A. Kazenin, "Limit problems of heat or mass transfer to a cylinder and a sphere immersed in an infiltrated granular bed," Prikl. Mekh. Tekh. Fiz., No. 5, 94-102 (1977).

2. H. S. Brinkman, "A calculation of the viscous force exerted by a flowing fluid on a dense swarm of particles," Appl. Sci. Res., **A1**, No. 1, 27-34 (1947).
3. V. A. Mukhin and N. N. Smirnova, "Investigation of heat and mass exchange processes in filtration of porous media," Novosibirsk (1978); Preprint, Inst. Termofiz., Sib. Otdel., Akad. Nauk SSSR, No. 26-78.
4. V. D. Zhak, V. A. Mukhin, V. E. Nakoryakov, and S. A. Safonov, "Propagation of a submerged jet in a narrow slot," Prikl. Mekh. Tekhn. Fiz., No. 3, 69-77 (1985).
5. A. V. Gorin, A. G. Khoruzhenko, and V. M. Chupin, "Natural convection from a heat source in a narrow slot," in: Hydrodynamics and Heat and Mass Exchange in Stationary Granular Beds," Collected Scientific Works [in Russian], Inst. Termofiz., Siber. Otdel. Akad. Nauk SSSR, Novosibirsk (1991), pp. 128-138.
6. S. S. Vorontsov, A. V. Gorin, V. E. Nakoryakov, et al., "Natural convection in a Hele–Shaw cell," Int. J. Heat Mass Transfer, **34**, No. 3, 703-709 (1991).
7. M. E. Shvets, "Solution of a problem for an equation of the parabolic type," PMM, **18**, No. 2, 243-244 (1954).
8. B. W. Thompson, "Secondary flow in a Hele–Shaw cell," J. Fluid Mech., **31**, Pt. 2, 379-395 (1968).
9. V. E. Nakoryakov, A. P. Burdukov, O. N. Kashinskii, and P. I. Geshev, "Electrodiffusion method for investigation of the local structure of turbulent flows," Inst. Termofiz., Siber. Otdel, Akad. Nauk SSSR, Novosibirsk (1986).
10. V. E. Nakoryakov, V. D. Zhak, and S. A. Safonov, "Flow in a Hele–Shaw cell at large velocities," Russian Journal of Engineering Thermophysics, **1**, No. 1, 1-23 (1991).
11. S. L. Gordon, J. S. Newman, and C. W. Tobias, "The role of ionic migration in electrolytic mass transport diffusivities of $Fe(CN)_6^{3-}$ and $Fe(CN)_6^{4-}$ in KOH and NaOH solutions," Ber. Buns. Gesel, Phys. Chem., **70**, No. 4, 414-420 (1966).
12. V. A. Mukhin, A. A. Voropaev, and V. V. Baluev, "Experimental investigation of surface friction in transverse flow around a cylinder in a granular medium," in: Hydrodynamics and Heat and Mass Exchange in Stationary Granular Beds, Collected Scientific Works, Inst. Termofiz., Siber. Otdel. Akad. Nauk SSSR [in Russian], Novosibirsk (1991), pp. 14-21.
13. B. E. Nakoryakov, V. A. Mukhin, V. V. Baluev, and A. A. Voropaev, "Transport processes in transverse flow around a cylinder by filtration flow in a stationary granular medium," in: Hydrodynamics and Heat and Mass Exchange in Stationary Granular Beds, Collected Scientific Works, Inst. Thermofiz. Siber. Otdel. Akad. Nauk SSSR [in Russian], Novosibirsk (1991), pp. 3-13.
14. M. É. Azrov and O. M. Todes, Hydraulic and Thermal Principles of Operation of Apparatus With Stationary and Boiling Granular Beds [in Russian], Khimiya, Leningrad (1968).
15. V. I. Volkov, V. A. Mukhin, and V. E. Nakoryakov, "Investigation of the flow structure in a porous medium," Zh. Prikl. Khim., No. 4, 838-842 (1981).